

Multi-phase (6-Phase & 12-Phase) Transmission Lines: Performance Characteristics

First A. Zakir Husain, Second B. Ravindra Kumar Singh, and Third C. Shri Niwas Tiwari

Abstract— Problems regarding power flow and stability, particularly the voltage stability are of vital importance at EHV (Extra High Voltage) and UHV (Ultra High Voltage) level because of its sensitivity with real and reactive power changes. The problem has been studied to a great extent in case of three-phase systems; however the multi-phase (phase order more than three) system has received little attention. An investigation of these aspects has been carried out in this paper by extending the well understood techniques of three-phase systems to multi-phase lines as well as construction of performance characteristic curves relating to power flow and voltage stability performance of such system. A quantitative and qualitative comparison of multiphase phase systems presented in the paper can be used for planning, development and design of multiphase transmission network

Keywords— Multi-phase, Power flow, Rights-of-way, Transmission lines.

I. INTRODUCTION

THE deregulation and competitive environment in the contemporary power system network are poised to a new scenario in terms of load and power flow conditions leading to problems of line capacity. In this regard multi-phase power transmission systems have been investigated [1]-[9] as potential alternative to increase transmission capacity without increasing system voltages which have already reached extremely high level i.e. EHV and UHV. Further, due to constraints on land availability and several environmental problems, a fresh and renewed interest set in motion in search of techniques and technologies for improvement in power carrying capacity of existing system by multi-phase systems keeping the same rights-of-way and it has been found that 6-phase and 12-phase in particular are quite promising.

The problems concerning power flow and stability, particularly voltage stability are of particular interest in EHV three-phase as well as multi-phase power systems because of its sensitivity with changes in real and reactive power. In this connection, a proper analysis is essential to observe the behavior of the system when real and reactive power changes in a given system. Voltage stability is obtained by keeping specified voltage magnitude within the set of operating limits

under steady state conditions. When the voltage stability limit is crossed, it is not possible to bring back the receiving end voltage at its nominal value even with any variation in reactive power. The problem has been studied to a great extent in case of three-phase systems [10]-[19]. However the multi-phase system has received little attention and needs similar study. This paper deals with investigation of these aspects by extending the well understood techniques of three-phase systems to multi-phase lines. A number of performance characteristic curves have been constructed relating to power flow and voltage stability of such system. Considering the multi-phase line as longitudinal or radial or the one linking to systems on either end, several performance characteristics such as, (i) load end real and reactive power operating contour maps, (ii) reactive power loss characteristics, (iii) voltage-power characteristics (under loading conditions), (iv) reactive power requirements characteristics, (v) optimal reactive power at voltage stability limit, (vi) shunt capacitive support at voltage stability limit using characteristic of voltage dependant load, and (vii) loadability curves are constructed. Employing a sample system a quantitative as well as qualitative analysis is carried out to highlight relative performances of such systems as compared to their three-phase counterparts. It is believed that such performance curves would be highly helpful in planning and evaluating performance of multi-phase as compared to conventional three-phase systems.

This paper is the extended version of our earlier reported work [9]. The paper is organized as follows: Various performance characteristics for multiphase transmission system have been derived and graphically analyzed in section III to compare the advantages and limitations of multiphase system with conventional three phase system. The analysis of reactive power requirement for voltage stability of multiphase and three phase system has been carried out in section IV. Loadability analysis of multiphase system with compensator has been reported in section V.

II. BASIC CIRCUIT MODEL AND SAMPLE SYSTEM

The basic circuit model with lumped parameters adopted for the appropriate characteristics analysis of un-compensated EHV power transmission system is represented on single phase equivalent basis as shown in Fig. 1. Let E_A and I_A represent the voltage and current at sending end whereas E_B and I_B are the voltage and currents at receiving end side. Y_T and Y_{SH} in Fig. 1 represent equivalent series and shunt admittance of an equivalent pi-model of the transmission line.

F. A. Zakir Husain is with the Department of Electrical Engineering, National Institute of Technology, Hamirpur, 177005 INDIA (phone: +91 9816056570; fax: 01972223834; e-mail: zahusain2@yahoo.com).

S. B. Ravindra Kumar Singh is with the Department of Electrical Engineering, Motilal Nehru National Institute of Technology Allahabad, 200004 India (e-mail: rksingh@mnnit.ac.in).

T. C. Shri Niwas Tiwari, LDC Institute of Technical Studies, Allahabad India (e-mail: sntiwari@rediffmail.com).

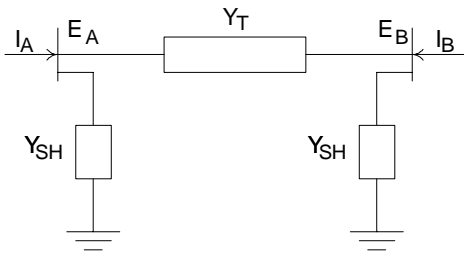


Fig.1 Basic circuit model

In order to construct and evaluate the appropriate characteristics curves, three transmission alternatives (3, 6 and 12-phase) with same number of conductors, same right of way and utilization of the same air space for power transmission are considered. Each system is energized at 462 kV line-to-ground (L-G) voltages and has the same thermal rating. The line-parameters are based on assumptions of complete transposition of conductors are depicted in Table 1.

TABLE I
TEST SYSTEM SPECIFICATION & LINE PARAMETERS

3-Phase line 462 kV (L-G)	6-Phase line 462 kV (L-G)	12-Phase line 462 kV (L-G)
SIL = 3275 MW	SIL = 4494 MW	SIL = 5485 MW
$Z=(0.0063+j0.398)$	$Z= 0.0126+j0.4726$	$Z=(0.025+j0.5667)$
Ω /mile	Ω /mile	Ω /mile
$Y=j10.638\mu S/mile$	$Y=j8.9606\mu S/mile$	$Y=j7.483\mu S/mile$

III. PERFORMANCE CHARACTERISTICS

A. Load End Real and Reactive Power Operating Contour Maps

With reference to Fig.1, load end real and reactive power operating contour maps [14] can be described by the following expression

$$|S_B| - |Y_{BB}^* E_B^2| = |e Y_{BB}^* E_B| \tag{1}$$

The above equation is an equation of a circle with $|Y_{BB}^* E_B^2|$ as centre and $|e^* Y_{BB}^* E_B|$ as its radius. Thus all states having the constant amplitudes of e ($= E_A Y_{BA} / Y_{BB}$) lie on the circles with these parameters on the S-plane (Fig. 2). Each circle (Fig. 2) represents the locus of $|S_B|$, the receiving end complex power, for a stable value of E_B (receiving end voltage), varying within the range of 0.95 p. u. to 1.05 p. u.

Employing (1) and assuming sending end voltage E_A to be constant at 1.0 p.u., the load end real and reactive power operating contour maps, for 3, 6 and 12-phase are constructed for 462 kV and 500 km transmission lines, on p.u. basis, are as shown in Fig. 2. It is evident from the curves in Fig. 2 that the power handling capacity of multi-phase (employing more than 3-phase) transmission system is higher for specified sending

end and receiving end voltages while maintaining the similar nature of variation.

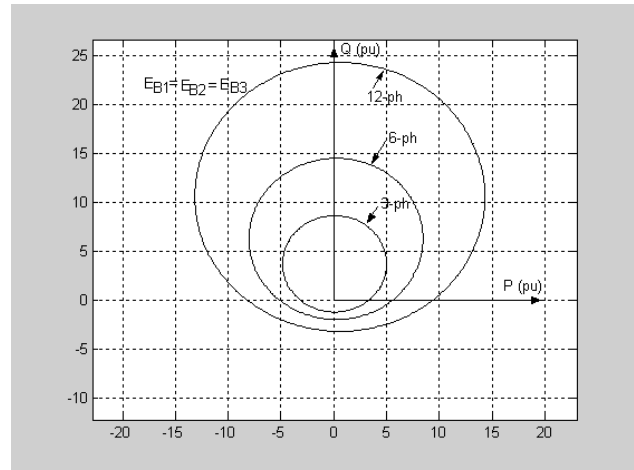


Fig. 2 Real & reactive power operating contours with same receiving end voltages ($E_B = 0.95$ p. u.)

Furthermore, Figs. 3(a-c) confirm enhancement of power handling capacity for 3, 6 and 12-phase transmission system with 5% increase of receiving end voltage $E_{B1} = 0.95$, $E_{B2} = 0.99$ and $E_{B3} = 1.05$ p.u. maintaining sending end voltage (E_A) as it is i.e. $E_A = 1.0$ p.u. It is observed that reactive and real power handling capacity for 3-phase, 6-phase and 12-phase systems are increased by 11.85 %, 8.33 %, 7.71 % and 5 %, 4.385 %, 4.384 % respectively. As supplement, it can be seen from Figs. 3(a-c) that increment in real and reactive power capacity for 3-phase, 6-phase and 12-phase takes place with an increase of 10 % in E_B (within voltage stable zone) keeping E_A constant at its previous value i.e. $E_A=1.0$ p.u.. It is observed that the corresponding percentage increase of in real and reactive power capacity of 3-phase, 6-phase and 12-phase are found to be 10, 8.77, 8.73 and 17.41, 13.88 and 15.40 respectively.

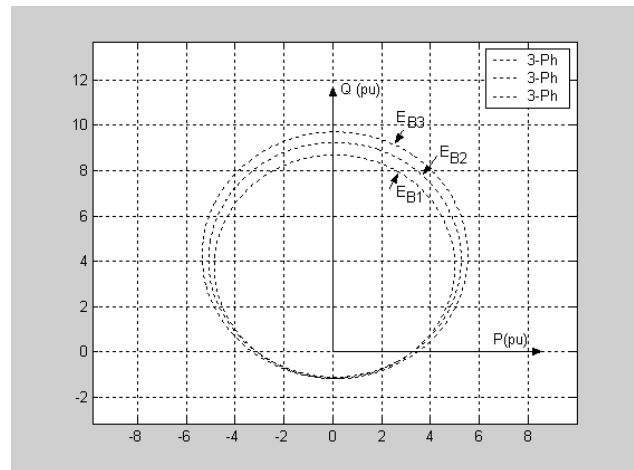


Fig. 3 (a) Real & reactive power contours of a 3-phase line with $E_{B1} = 0.95$, $E_{B2} = 0.99$ and $E_{B3} = 1.05$ p.u.

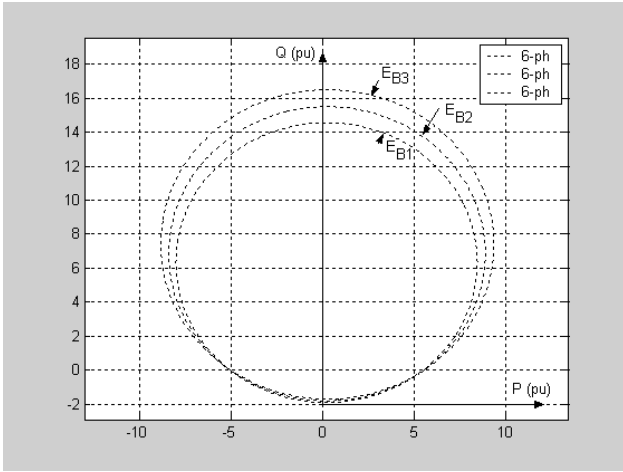


Fig.3 (b) Real & reactive power contour maps of a 6-phase line with $E_{B1} = 0.95$, $E_{B2} = 0.99$ and $E_{B3} = 1.05$ p.u

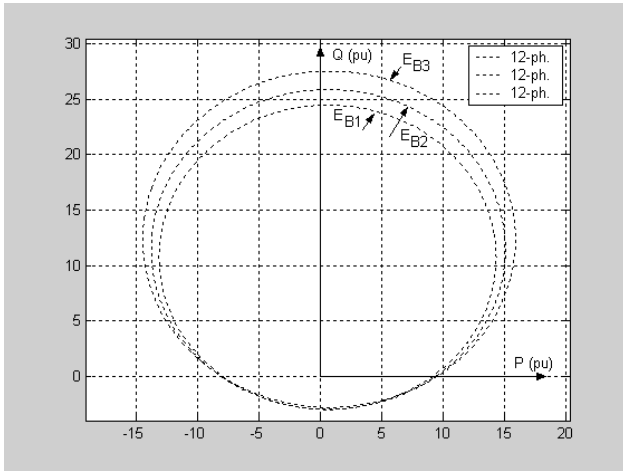


Fig.3 (b) Real & reactive power contour maps of a 12-phase line with $E_{B1} = 0.95$, $E_{B2} = 0.99$ and $E_{B3} = 1.05$ p.u

It is evident from the above contour maps that the reactive power transfer capacity increases with the increase of number of phases. Thus it can be inferred from the load end real and reactive power counter maps that the multi-phase transmission systems will be inherently more stable from voltage stability point of view than the traditional three-phase transmission systems.

B. Reactive Power Loss Characteristic

The net series reactive losses (Q_{SL}) in an EHV power transmission line are described by

$$Q_{SL} = I^2 X = \left(\frac{(Q_{SL0} = E_B I_B)}{E_B} \right)^2 X \tag{2}$$

For the assumed constant power ($Q_{SL0} = E_B I_B$), the rate of change of series reactive power losses with voltage is obtained from (2) as:

$$\frac{dQ_{SL}}{dV} = \frac{-2(Q_{SL0})^2 X}{E_B^3} \tag{3}$$

It is evident from (3) that rate of change of reactive power loss with respect to receiving end voltage is inversely proportional of the cube of receiving end voltage. Therefore, an increment in series reactive power losses (dQ_{SL}) would be possible with a decline in the transmission voltage in order of E_B^3 . Employing (3) curves of (dQ_{SL} / dE_B) versus E_B (p.u.) are drawn for the sample cases of 3, 6 and 12-phase lines and depicted in Fig. 4 for a length of 500 km.

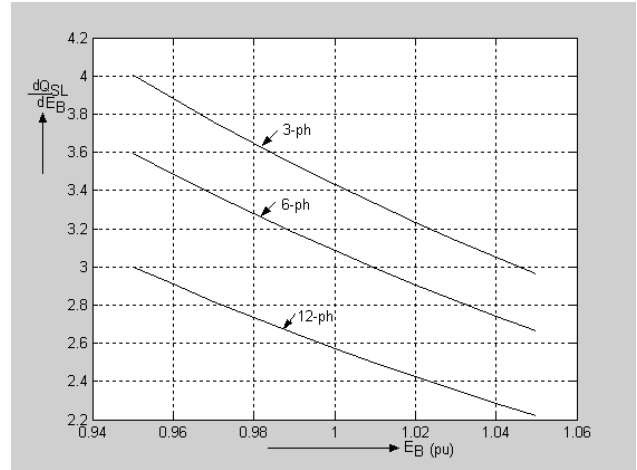


Fig. 4 Reactive power loss characteristics of three transmission alternatives

From the curves in Fig. 4, it is observed that the series reactive power losses are relatively lesser in multi-phase transmission lines than that in its three-phase counterpart. This implies that the voltage stability limit of multi-phase transmission systems will be increased, making multi-phase systems more secured from the voltage stability view point. Equation (2) can further be written as

$$Q_{SL} = (E_B I_A)^2 \left(\frac{1}{E_B / X} \right) = \frac{(E_B I_B)^2}{SIL} \tag{4}$$

where, SIL is the surge impedance loading and is given by E_B^2 / X . Based on (4) the results are shown in the plots of QSL versus SIL vide Fig. 5 for a length of 500 km.

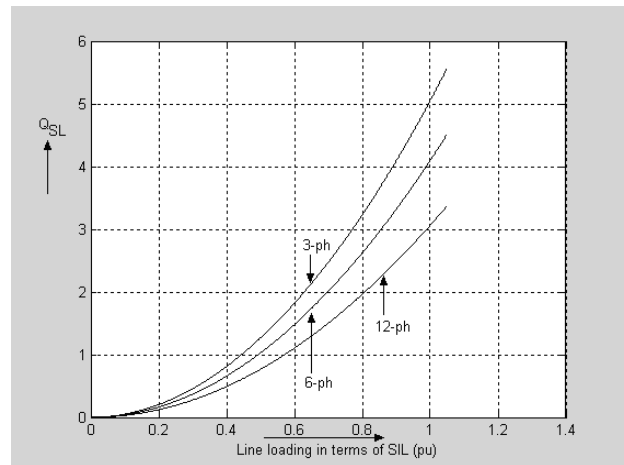


Fig. 5 Profile of series reactive power losses (Q_{SL}) verses surge impedance loading (SIL).

It is also evident from Fig. 5 that the reactive power losses are comparatively lesser in multi-phase lines than that of its 3-phase counterpart. In view of this, multi-phase systems (employing more phases than three) will be more secured from voltage stability view point.

C. Voltage- Power Characteristics

If a power transmission line is assumed to be lossless, then the sending and receiving end voltages can be expressed as follow [17]-[19]:

$$E_A = E_B \cos \theta + jZ_c \sin \theta \left(\frac{P_B - jQ_B}{E_B} \right) \quad (5)$$

Equation (5) on simplification becomes

$$E_B = \frac{E_A \pm (E_A^2 - 2Z_c P_B (\sin 2\theta))^{0.5}}{2 \cos \theta} \quad (6)$$

Where Z_c is characteristic impedance and θ is electrical line length expressed as 0.0743ohms/ km. The expression vide (6) indicates that if sending end voltage is fixed ($E_A=1.0$ p.u.), the receiving end voltage varies with load power factor and line length. Making the use of (6), the P_B - E_B curves are constructed in Figs. 6(a-c) for three alternative transmission systems i. e. 3, 6 and 12-phases assuming line length 500 Km. These figures represent the plots between receiving end voltage and power under specified operating conditions. From Figs. 6(a-c), it is observed that for each load power factor the maximum receiving end power is found largest for 12-phase power transmission system.

Thus it can be concluded that with increase number of phase maximum power at the receiving end will be progressively enhanced maintaining the voltage stability at various power factor of the load. The above statement is also true for specified load power factor and varying the length of transmission systems, which is clearly visible through Figs. 7 (a -b)

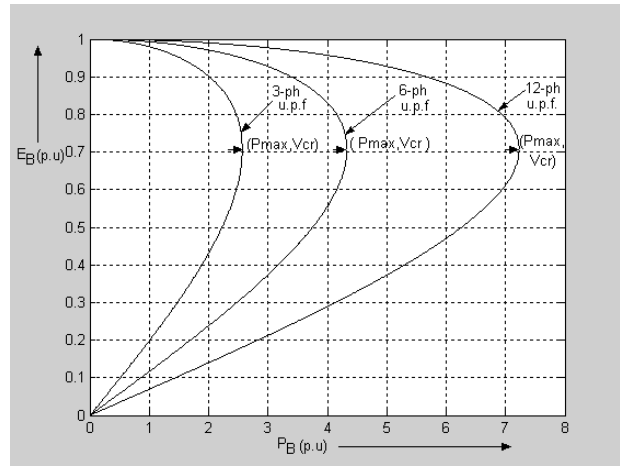


Fig. 6 (b) Receiving end voltage profile for varying power flow at p.f. u. for a 500 km line

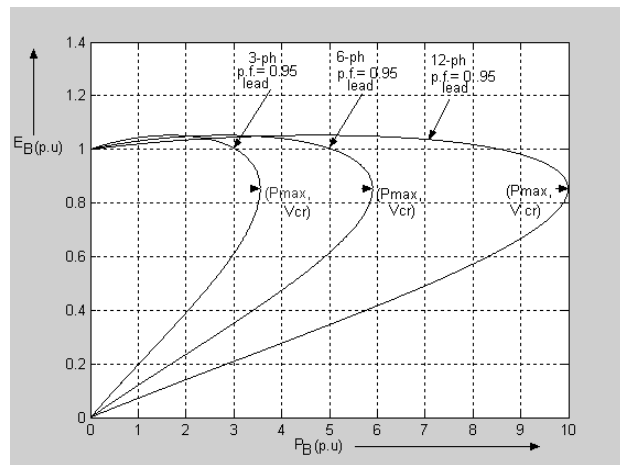


Fig. 6(c) Receiving end voltage profile for varying power flow at p.f. 0.95 lead for a 500 km line

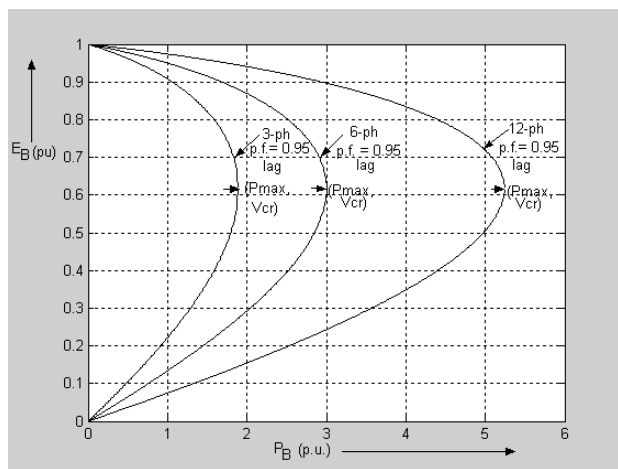


Fig. 6 (a) Receiving end voltage profile for varying power flow at p.f. 0.95 lag for a 500 km lin

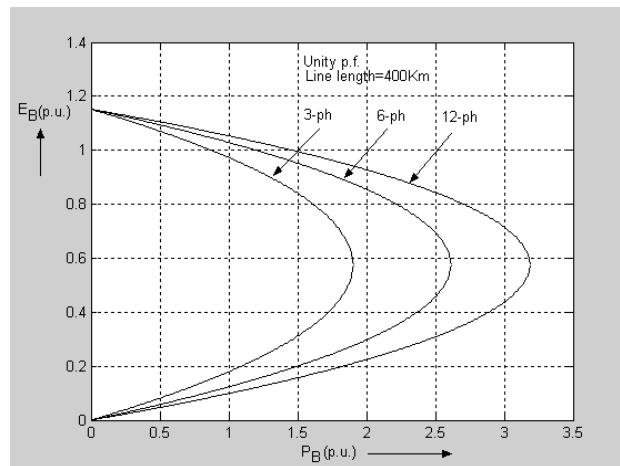


Fig.7 (a) Relationship between receiving end voltage and power at u.p.f and line length of 400 km.

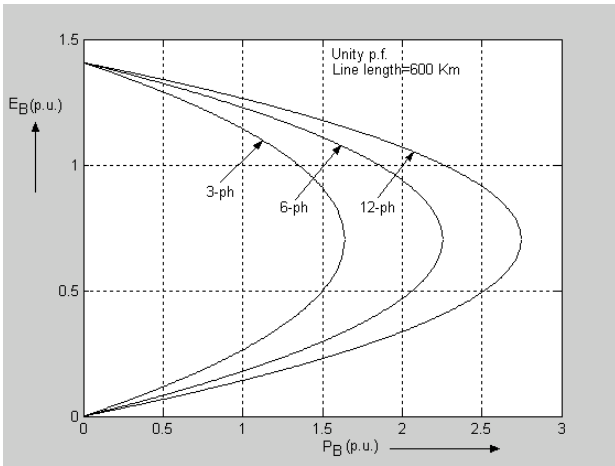


Fig. 7 (b) Relationship between receiving end voltage and power at u.p.f and line length of 600 km.

IV. ANALYSES OF REACTIVE POWER REQUIREMENTS

Assuming E_A leads E_B by an angle δ , E_A can be written as

$$E_A^{j\delta} = E_A (\cos \delta + j \sin \delta) \quad (7)$$

Substituting (7) in (5) and equating real and imaginary parts of the resulting equation, the relationship between receiving end reactive power and voltages can be written as

$$Q_B = \frac{E_B (E_B \cos \delta - E_A \cos \theta)}{Z_C \sin \theta} \quad (8)$$

Similarly,

$$Q_A = -E_A (E_B \cos \delta - E_A \cos \theta) / Z_C \sin \theta \quad (9)$$

If $E_A = E_B$ then

$$Q_B = -Q_A = E_A^2 (\cos \delta - \cos \theta) / Z_C \sin \theta \quad (10)$$

For lossless line, $\cos \theta = 1$, (10) reduces to

$$Q_B = E_A^2 (1 - \cos \delta) / Z_C \sin \theta \quad (11)$$

where δ is the transmission angle, Z_C is the characteristic impedance and θ is electrical line length expressed as 0.0013 rad./ km. Employing (11) the terminal reactive power curves as a function of power transmitted for different line length are constructed in Figs. 8(a-b)

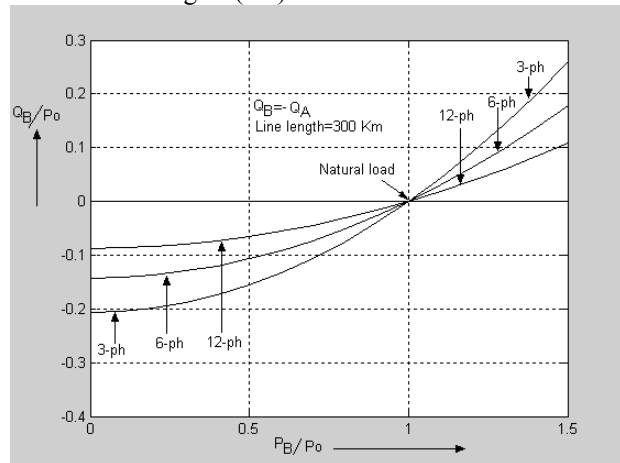


Fig. 8 (a) Terminal reactive power as a function of power transmitted for 300 km lines

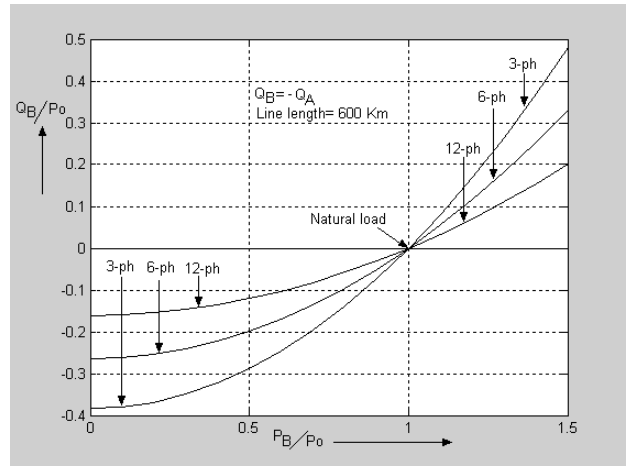


Fig. 8 (b) Terminal reactive power as a function of power transmitted for 600 km lines.

Figs. 8 (a-b) represent the curves between per unit reactive power and per unit active power for several lengths of 3-phase, 6-phase and 12-phase transmission systems respectively. From examination of these curves, the following observations and conclusions can be derived.

When $P_B < P_0$ (SIL), there is obviously an excess of line charging found. As a result, Q_A is found negative and Q_B is obtained positive. This clearly indicates that the reactive power is being absorbed by the system at both ends. Therefore a reactive (inductive) compensation is essential for maintaining the voltage stability.

While $P_B > P_0$, reactive power is being generated at both ends. Obviously lagging power factor operation is inevitable. Hence, capacitive compensation is needed for maintaining the voltage stability of the system.

Now from the above comparative analysis of the Figs. 8 (a) & (b), it is clearly evident that the reactive power requirement to maintain stable voltage varying load is least for highest multi-phase system (12-phase). In other words as the phase order increases, the requirement of reactive power is reduced gradually for different transmission line lengths. This also implies that the rating of the compensating devices for multi-phase system will be lower as compared to their lower phase order counterparts

A. Optimal Reactive Power at Voltage Stability Limit

In the lossless line case, the power flow equations can be written as

$$P_B = \frac{E_A E_B}{X} \sin \delta \quad (12a)$$

$$Q_B = \frac{E_A E_B}{X} \cos \delta - \frac{E_B}{X} \quad (12b)$$

The determinant of the Jacobian [19] of load flow equations in a loss less network is given by

$$\Delta[J] = \frac{1}{X} (-E_A E_B + 2E_B^2 E_A \cos \delta) \quad (13)$$

with $\Delta[J] = 0$ at voltage stability limit, the receiving end voltage can be written as

$$E_A = 2E_B \cos \delta \tag{14}$$

Using (14) in (12b), the value of reactive power at the limiting stage of voltage stability is given by

$$Q_{lim} = \frac{E_B^2}{X} \cos 2\delta \tag{15}$$

where, Q_{lim} represents the limiting value of reactive power transfer in a transmission system and it is critical value for voltage breakdown.

A study of Q_{lim} with respect to E_B has been carried out employing (15) and it is illustrated through plots in Fig. 9. This figure (Fig. 9) indicates that the reactive power limit for maintaining the voltage stability at different receiving end voltages for transmission line of length of 500 Km with the range of variation from 1.0 pu. to 0.90 p.u.. The curves shown in Fig. 9 are obtained for various transmission systems i.e. 3, 6 and 12-phase. Over and above it is further observed that the reactive power limit is gradually reducing as the phase-order is increasing from 3-phase to 12-phase at each and every point of per unit receiving end voltage within the range from 1.0 p.u. to 0.90 p.u. Under the circumstances, with increase of number of phases the rating of the devices required from the point of view of compensation is gradually diminished. This also implies that the even in uncompensated mode, the higher phase order system performs well from the voltage stability view point since the requirement of reactive power is gradually reduced.

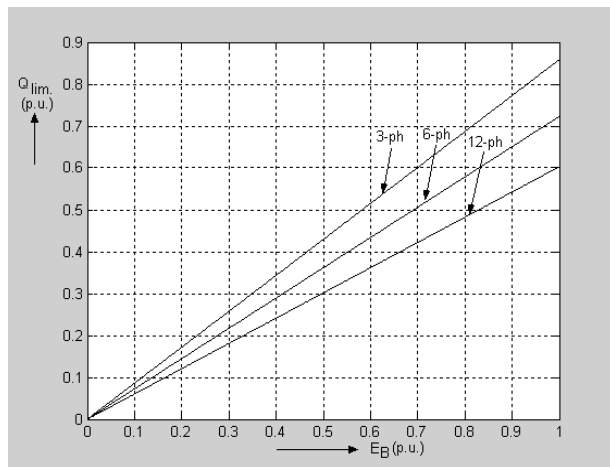


Fig. 9 Reactive power limit profile for various systems to have voltage stability for different receiving end voltages

B. Shunt Compensation for Voltage Stability

Shunt capacity support at voltage stability limit using characteristics of voltage dependent load [14] is illustrated by the following equation

$$|Y_{SH}| = \frac{|E_A| |Y_{BA}|}{m P_0 |E_B^{m-1} | \sec \phi - 2 |E_B|} - |Y_T| \tag{16}$$

where P_0 is the power at rated voltage E_B and m is the load characteristics for the voltage dependant loads.

Equation (16) provides a relationship for the minimum of Y_{SH} at load end for getting a stable voltage state under set of specified operating conditions. Figs. 10 (a) and (b) exhibit the magnitude of the minimum receiving end bus admittance at different per unit voltages for different power factors in case of multi-phase systems (3, 6 and 12-phase). The above cases are shown for $m = 0.5$ and $m = 1.0$. It is observed that enhancement of shunt capacitive support is required to improve the receiving end voltage magnitude from the point of view of the stability of the system voltage in case of voltage dependent load (i. e. $m < 1$). It is further clarified that the requirement of shunt capacitive support rating for voltage dependent load is gradually reduced as the phase-order of the system is increased from 3 to 12.

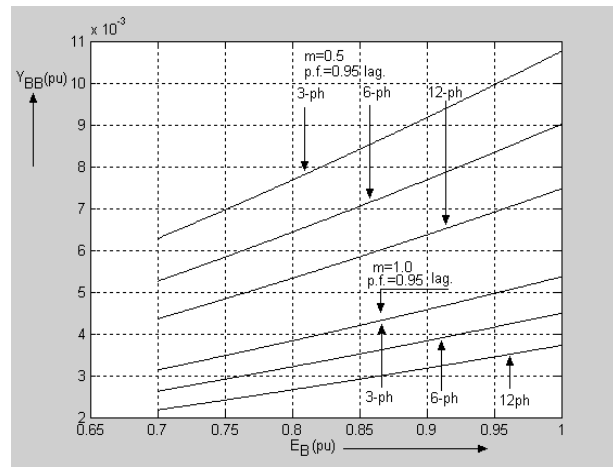


Fig.10 (a) Profile of minimum magnitude of load end bus admittance at different voltages with 0.95 p.f. lagging at voltage stable states

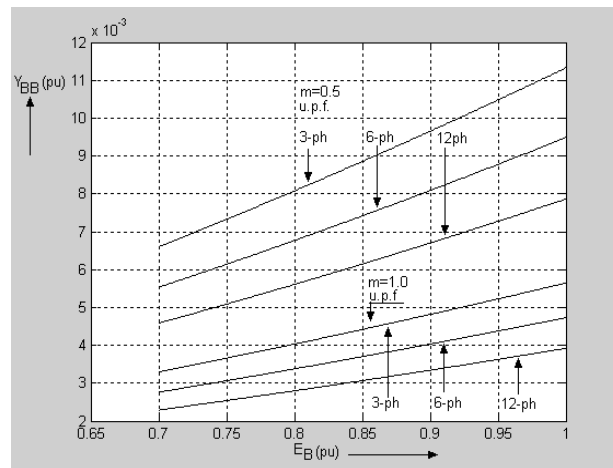


Fig.10 (b) profile of minimum magnitude of load end admittance at different voltage with u.p.f. at voltage stable state

The same analysis has been carried for variation of length of transmission line and it has been given in Fig. 11. For analysis, in place of the variation of receiving end voltage, the length of transmission line is varied and the similar curves are drawn, then the same observations are noticed. Figs. 11 (a) and (b) represent the curves - shunt admittance ($Y_{SH} = Y'_{BB}$) versus length (L) for different power factors (0.95 lagging & unity) at $m = 0.5$ and $m = 1$ in case various multi-phase transmission systems (3, 6 and 12 -phase). It can be concluded that with increase of number of phases the value of the shunt capacitive rating is reduced for voltage dependent load at voltage stability limit.

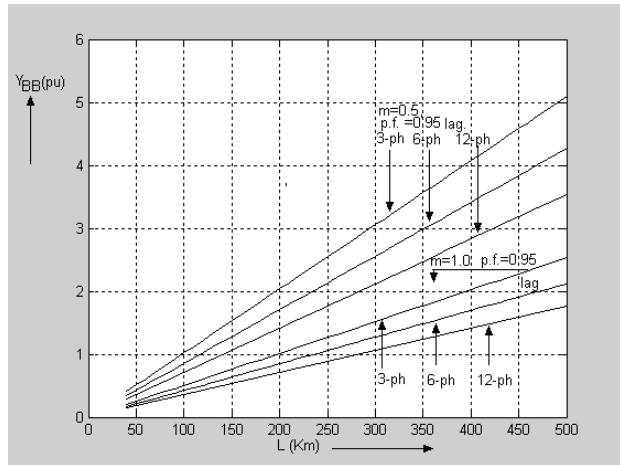


Fig. 11(a) Profile of load end admittance for varying line length with p.f.0.95 lag at voltage stability limit.

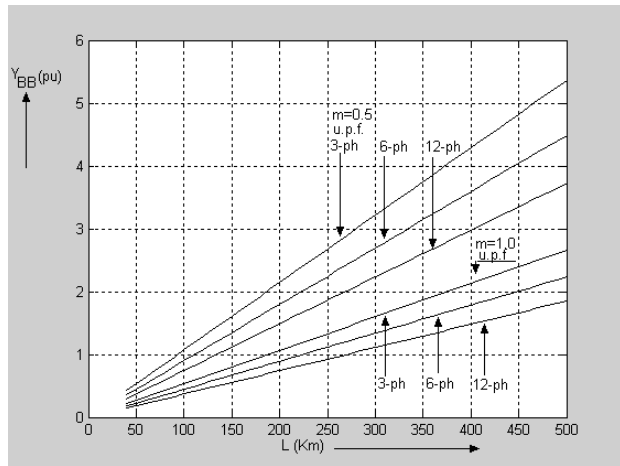


Fig. 11 (b) Profile of load end admittance for varying line length with u.p.f. at voltage stability limit.

V. LOADABILITY CHARACTERISTICS FOR SERIES COMPENSATED LINE

The equivalent series circuit of multi-phase transmission line with series compensator (for example a thyristor controlled series compensator (TCSC)) is shown in Fig. 12. It has been

assumed in the analysis that capacitive compensation of the transmission line has been carried out, although both capacitive and inductive compensation are possible. In a practical system, a capacitive compensation is more practical and therefore the characterization has been carried for this only in this paper.

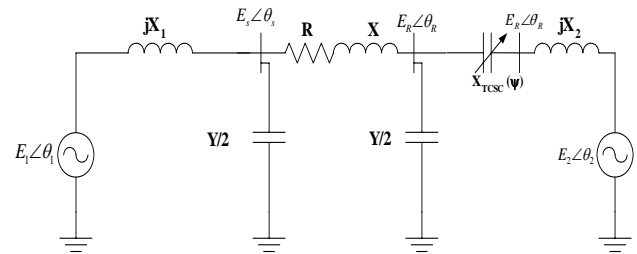


Fig. 12 circuit model for power and loadability study.

The power flow at sending end bus the can be written and computed as follows.

$$P_S = |E_S||E_R| \cos(\beta + \delta) / |B| + |A||E_S|^2 \sin(\beta - \alpha) / |B| = P_A \tag{17}$$

where A & B are the generalized parameters of the transmission network including compensation device $X_{TCSC}(\psi)$ and δ is the angle between voltages E_S and E_R [9]. The P_A divided by SIL yields the loadability in per unit. Ψ degree of compensation is shown in Table 2

TABLE 2
Ψ DEGREE OF COMPENSATION

Deg. of Compensation	3-phase		6-phase		12-phase	
	Ψ(deg ree)	$X_{TCSC(\psi)}$	Ψ(deg ree)	$X_{TCSC(\psi)}$	Ψ(deg ree)	$X_{TCSC(\psi)}$
25%	51.60	0.0995	51..60	0.1181	51..60	0.1415
50%	40.56	0.1990	40..56	0.2363	40..56	0.2800
75%	36.99	0.2985	36..99	0.3544	36..99	0.4245

A. Line Loadability Analysis

For the model shown in Fig. 12, the transmission line is represented by an equivalent π model with the terminals (sending and receiving ends) as Thevian's equivalents [20], [21] whereas the model of TCSC [9] as series resistance and reactance of the line. The transmission line consists of positive sequence inductive and capacitive parameters. The Thevian's equivalent impedances are determined from short circuit strengths of the systems and the voltages $|E_1|$ and $|E_2|$ are specified as 1.0 and 9.7 p.u. respectively based on A.C. load flow. The power flow and loadability analysis are carried out on three transmission alternatives namely 3-phase, 6-phase and 12-phase for which system voltage is 462 kV, L-G. The specification of 3-phase, 6-phase and 12-phase used as sample system are given in Table 1.

B. Line Loadability Analysis

The power flow and loadability analyses are carried out on three alternatives as described in Table 1. Initially power flow for uncompensated line (250 km length) and employing various degree of compensation for three alternatives transmission system (3, 6 and 12-phase) are computed, recorded and plotted as shown in Figs. 13(a-d). Next, with all known voltages and other parameters mentioned above, the ratio P_A/SIL for uncompensated and various degree of compensation for the three alternatives, for 5% voltage drop and 30% stability margin criteria, have been plotted against line length between 100 and 600 miles as shown in Figs. 14. The loadability characteristics depicted in Fig. 14 (a-d) are used to study qualitative and quantitative benefits in each case.

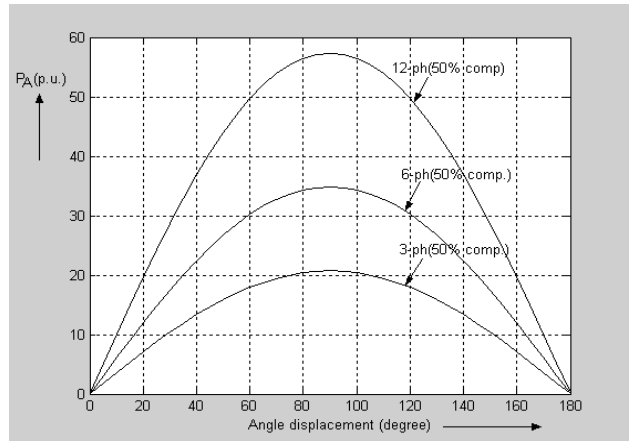


Fig. 13 (c) Power-angle curve for line length 250 km with 50% compensation

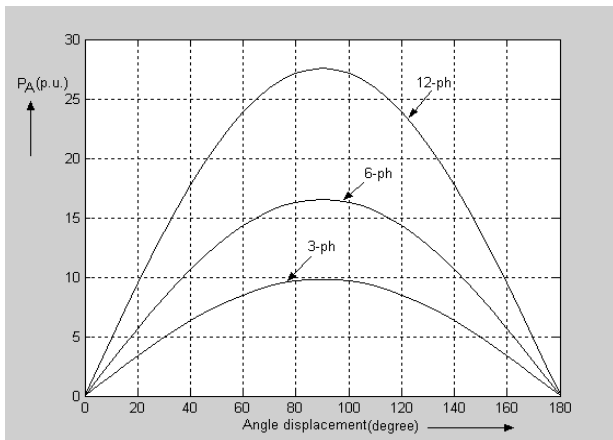


Fig. 13 (a) Power-angle curve for line length 250 km with no compensation.

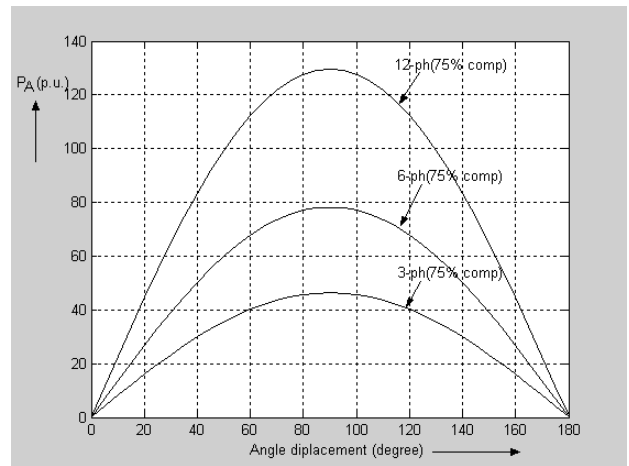


Fig. 13 (d) Power-angle curve for line length 250 km with 75% compensation.

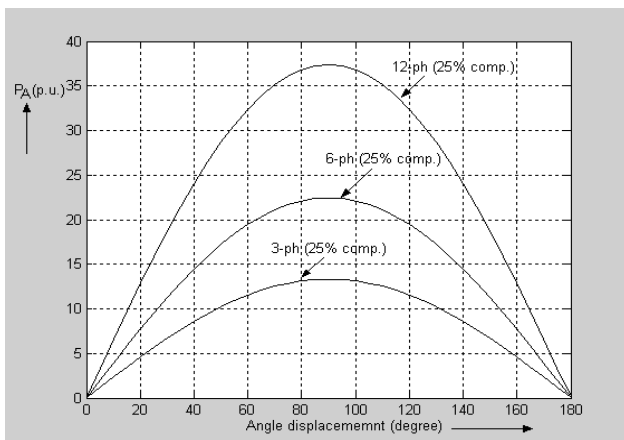


Fig. 13 (b) Power-angle curve for line length 250 km with 25% compensation

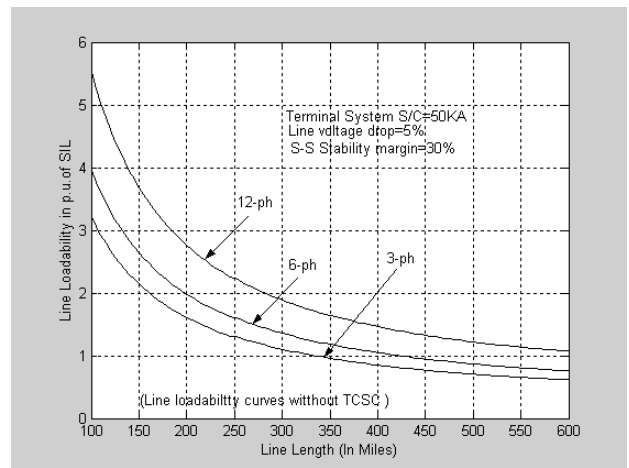


Fig. 14 (a) Loadability curves for three alternative lines (3-phase, 6-phase & 12-phase) with no compensation

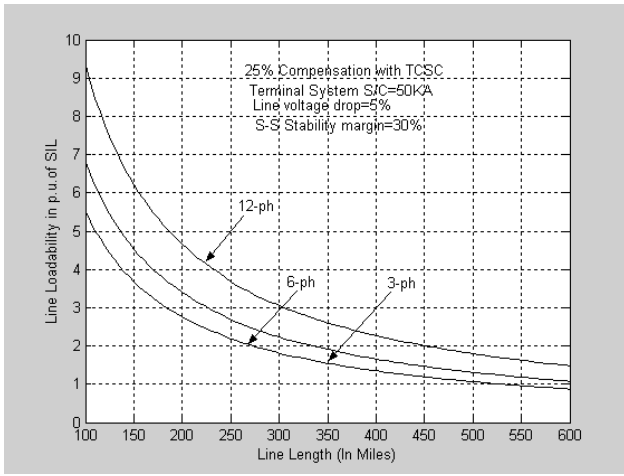


Fig.14 (b) Loadability curves for three alternatives lines (3-phase, 6-phase & 12-phase) with 25 % compensation.

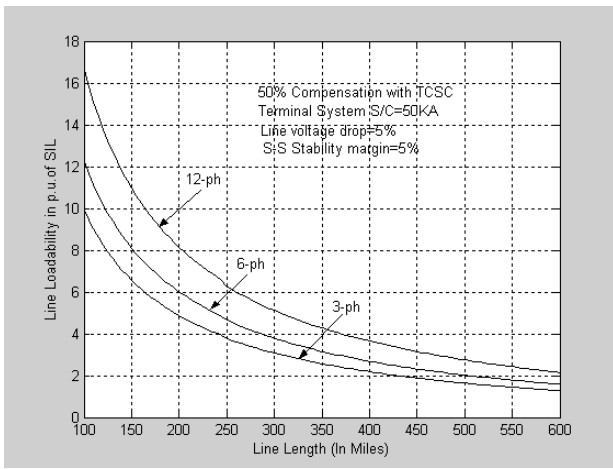


Fig.14 (c) Loadability curves for three alternatives lines (3-phase, 6-phase & 12-phase) with 50 % compensation.

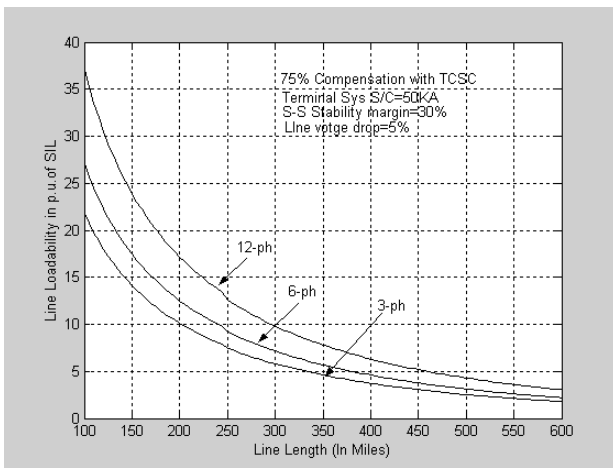


Fig. 14 (d) Loadability curves for three alternatives lines (3-phase, 6-phase & 12-phase) with 75% compensation.

It is to be noted that the power flow and loadability analysis has been carried out on three transmission alternatives described in Table 1. The power flow for the case of uncompensated line (250 km length) and employing various degree of compensation are calculated and plotted as in Fig.13 (a-d). It is evident from Figs. 13 (a-d) that steady-state stability limit (Pmax) as shown in Figs.13 (a-d) called steady state limit) is higher for multi-phase lines as compared to its 3-phase counterpart. The loadability studied for uncompensated line as well as compensated line with several degree of compensation (by varying $X_{TCSC(\psi)}$) revealed remarkable benefits as evident from Fig. 14 in line loadability of multi-phase lines than its lower phase counterpart

VI. CONCLUSION

In this paper the existing 3-phase concepts have been extended and employed to construct and analyze various performance characteristics curves on power flow and voltage stability of the multi-phase line. Based on the investigations of 6-phase and 12-phase transmission lines and their comparison with the conventional 3-phase system, following conclusion may be made.

The multi-phase lines (6-phase and 12-phase) show progressively increased power handling capacity, reduced reactive power losses, increased power at the receiving end, reduced reactive power requirement for maintaining stable load voltage, reduced rating of compensating devices, better voltage stability in case of voltage dependent load and increased line loadability in uncompensated as well as compensated condition as the phase order is increased. These aspects of multi-phase lines may be very attractive and beneficial to electric transmission utility.

REFERENCES

- [1] L. O. Barthold and H. C. Barnes, *High phase order power transmission*, *Electra*, Vol. 24, 1972, pp.-139-153.
- [2] J.R. Stewart and D.D. Wilson, *High phase order transmission—a feasibility analyses part-I steady state considerations*, *IEEE Trans. PAS-97*, 1978, pp. 2300-2307
- [3] S.N. Tiwari, G.K. Singh and A.S. Bin Saroor, *Multi-phase transmission research—a survey*, *Electr. Power Syst. Res.*, (24), 1992, pp.207-215.
- [4] T. L. Landers R.J. Richeda, E. Krizanskas, J.R. Stewart, and R.A. Brown, *High phase order economics: constructing a new transmission line*, *IEEE Trans. PWRD-13*, No.4, 1998, pp.1521-1526
- [5] I.A. Metawally, *Electrostatic and environmental analyses of high phase order transmission lines*, *Electr. Power Syst. Res.* 61(2), 2002, pp. 149-159
- [6] R. Billinton, S.O. Fareed and M.F. Firuzabad, *Composite system reliability evaluation incorporating a six-phase transmission line*, *IEE Proc.*, Vol. 150, No.4, 2003, pp. 413-419.
- [7] H. Elrefale, *Modeling arching faults of six-phase transmission lines*, *IEE Conf.*, 2004, pp. 48-51
- [8] M.W. Mustafa, M.R. Ahmed and H. Shareef, *Fault analysis on double three-phase to six-phase converted transmission line*, *IEEE Power Engg. Conference, IPBC*, 2005, pp. 1-5
- [9] Zakir Husain, R.K. Singh, and S.N. Tiwari *Multi-phase (6-phase & 12-phase) power transmission systems with thyristor controlled series capacitor*, *Proc. Of the 6th WSEAS Int. Conf. On Application of Electrical Engg. (AEE '07)*, 2007, pp. 246-250.

- [10] F.D. Glaliana and Jargis, *Quantitative analysis by steady state stability in power networks*, IEEE Trans. On P.A & S. Vol. PAS-100, No.1, 1981, pp.318-326.
- [11] S. Abe, Y. Fukunaga, A. Isono and B. Kondo, *Power system voltage stability*, IEEE Trans. On P.A. & S. Vol. PAS-101, No.10, 1982, pp.3830-3840.
- [12] Y. Tamura, M. Mori and S.Iwamoto, *Relationship between voltage stability and multiple load flow solution in electric power systems*, IEEE Trans. On P.A. & S. Vol. PAS-102, No, 5, 1983, pp. 1115-1125.
- [13] C.S. Indulkar and B. Viswanathan, *Effect of series compensation on the voltage instability EHV long lines*, Electr. Power Syst. Reas., No.6, 1983, pp.185-191.
- [14] A. Chakrabarti and A.K. Mukopadhay, *Load end real and reactive power operating contour and shunt capacitive support at voltage stability limit of an E.H.V power system*, Proc. SICE-IEEE KAAC International conference Japan, 1989, pp.1001-1003.
- [15] M.R. Aghamohammadi and M. Mohammadian, *Sensitivity characteristic of neural network as a tool for analyzing and improving voltage stability*, Proc. IEEE Conf., 2002, pp.1128-1132.
- [16] H. Sun, X. Zhou and R. Li, *Accuracy analysis of static voltage stability indices based on power flow model*, Proc. IEEE Conf., 2005, pp1-7
- [17] T.J.E. Miller, *Reactive power control in electric systems*, 1st ed., John Wiley, 1982, pp. 67-82
- [18] P. Kundur, *Power system stability and control*, 1st ed., McGra-Hill, New York, 1993, pp. 216-225
- [19] A. Chakrabarti, D.P. Kothri and A.K. Mukhopadhyay, *Performance, operation and control of E.H.V. Power Transmission Systems*, 1st ed., Wheeler, 1995. pp. 51-160
- [20] R.D. Dunlop, R.Gautam and P.P. Machenko, *Analytical development of loadability characteristics for EHV and UHV transmission lines*, IEEE Trans.Vol. PAS-98, 1979, pp. 606-617.
- [21] R. Gautam, *Application of line loadability concepts to operating studies*, IEEE Trans. Vol. PWRS-3, No.4, 1988, pp. 1426-1433